Effect of biomass fuel ash and bed material on the product gas composition in DFB steam gasification

K. Fürsatz [a, b, *], J. Fuchs [b], F. Benedikt [b], M. Kuba [a, b, **], H. Hofbauer [b]

[a] BEST – Bioenergy and Sustainable Technologies GmbH, Inffeldgasse 21b, 8010, Graz, Austria
[b] TU Wien, Institute of Chemical, Environmental and Bioscience Engineering (ICEBE), Getreidemarkt 9/166, 1060, Vienna, Austria

ARTICLE INFO

ABSTRACT

Gasification is a thermochemical process that transforms carbonaceous matter into a gaseous secondary energy carrier, referred to as product gas. This product gas can be used for heat and power generation but also for syntheses. One possible gasification technology suitable for further synthesis is dual fluidised bed (DFB) steam gasification. The H_2:CO ratio, which determines the suitability of the product gas for further synthesis, is influenced by the catalytic activity inside the gasification reactor. Eleven DFB steam gasification experiments were performed comparing the catalytic activity for various bed material and fuel combinations. The bed materials used were K-feldspar, fresh and layered olivine, and limestone, and the fuels gasified were softwood, chicken manure, a bark–chicken manure mixture and a bark-straw-chicken manure mixture. The water-gas-shift (WGS) equilibrium deviation was used to evaluate the catalytic activity inside the gasification reactor. It was shown that both the fuel ash and bed material have an effect on the catalytic activity during gasification. Scanning electron microscopy and energy dispersive X-ray spectrometry showed the initial layer formation for experiments with ash-rich fuels. Isolated WGS experiments were performed to further highlight the influence of bed material, fuel ash and fuel ash layers on the WGS equilibrium.

© 2020 The Author(s). Published by Elsevier Ltd. This is an open access article under the CC BY license (http://creativecommons.org/licenses/by/4.0/).

1. Introduction

During gasification carbonaceous matter is converted into a product gas mainly consisting of H_2, CO, CO_2, CH_4, C_2H_4 and H_2O. Product gas can be used for heat and power production [1,2], H_2 can be separated [3] or products like Fischer-Tropsch diesel [4], synthetic natural gas [5,6] and mixed alcohols [7,8] can be synthesised, making product gas a flexible secondary energy carrier. In times of oil scarcity (e.g. Second World War, 1973 oil embargo), coal gasification was a suitable alternative for the production of liquid transportation fuels [9]. Today, the increasing desire to reduce the use of fossil fuels is giving new momentum to the development of gasification technologies, this time using biomass and residues as fuel.

During dual fluidised bed (DFB) steam gasification it is possible to reach a H_2:CO ratio of 2 in the product gas directly after gasification [10]. DFB steam gasification consists of two interconnected fluidised beds, the gasification reactor (GR) and the combustion reactor (CR). Fluidised beds consist of a so-called bed material and a fluid which is passed up through the bed material. In the right conditions, the bed material is suspended in the fluid and the bed shows a behaviour similar to a fluid. In DFB steam gasification the bed material is transported between the two reactors to transport heat from the CR to the GR. The bed material additionally acts as a catalyst during gasification.

Researchers normally quantify the performance during gasification by char conversion [11,12], product gas composition [13,14] (often with a focus on H_2 [15] or tar content [16]) and/or the H_2:CO ratio [13]. Choosing these parameters as indicators of catalytic activity makes it challenging to compare experiments performed at different process conditions like varying temperatures, gasification medium and fuel feed. Especially the gasification temperature has a significant influence on the product gas composition and the H_2:CO ratio by influencing the kinetics as well as the reaction equilibria of the wide variety of reactions that occur during gasification.

---

* Corresponding author. BEST – Bioenergy and Sustainable Technologies GmbH, Inffeldgasse 21b, 8010, Graz, Austria.
** Corresponding author. BEST – Bioenergy and Sustainable Technologies GmbH, Inffeldgasse 21b, 8010, Graz, Austria.
E-mail addresses: katharina.fuersatz@best-research.eu (K. Fürsatz), matthias.kuba@best-research.eu (M. Kuba).

Choosing the deviation from a reaction equilibrium counters some of the aforementioned problems, making it easier to compare experiments performed at different conditions. Some of the most prevalent reactions during gasification are the Boudouard reaction [11,14,17] and the water-gas-shift (WGS) reaction [18,19]. The Boudouard reaction is of particular importance when gasifying pyrolysis char [11] or using CO_2 as the gasification medium [14]. Meanwhile, in the case of DFB steam gasification, the WGS equilibrium is particularly suitable to quantify performance since it gives the equilibrium between H_2O (the gasification medium), and H_2 and CO, the gas components especially relevant for downstream synthesis and was shown to be one of the major reactions occurring [18].

The normally used, catalytically active, bed material olivine contains heavy metals (e.g. nickel and chromium), which makes it necessary to deposit the ash accumulating during DFB steam gasification — a costly process [20]. Other catalytically active bed materials like dolomite [21–23] and calcite [24–26] are promising candidates to replace olivine as bed material. These materials have a low hardness [27], resulting in higher attrition of the bed material and consequently increased amounts of dust in the product gas [24]. More attrition-resistant minerals like quartz [24,28,29] and K-feldspar (K-FS) [24,30] have also been tested for their suitability in DFB gasification. However, these minerals have been found to only show little catalytic activity [24,31,32].

Interactions of fuel ash with bed material leads to layer formation around the bed particles [33]. This was associated with increasing the catalytic activity of the bed material in commercial plants [34]. Layers on inactive bed materials like quartz and K-FS were also proven to increase the catalytic activity [32,35,36]. Research focused on different residual fuels has shown that the composition of the layer forming on the bed material is influenced by the fuel ash composition [37] and is similar to the ash present in the system [38]. Residual fuels with higher ash contents (e.g. manures) speed up the layer formation and consequently the catalytic activation of the bed material [35]. Though special attention has to be given to agglomeration [39,40] and ash accumulation [41], which can both lead to fluidization problems and plant shut-downs, when using ash-rich fuels.

The aim of this work is to compare the impact of catalytically active bed materials to the impact of fuel ash and ash layers on the catalytic activity observed during DFB steam gasification. The catalytic activity is quantified by the WGS equilibrium deviation instead of the product gas composition to counteract small differences in the gasification temperature. Four fuels and four bed materials were experimentally investigated in various combinations in a 100 kW DFB steam gasification pilot plant. The results were further validated by isolated WGS experiments with fresh bed material and bed material samples, highlighting the importance of the WGS equilibrium for gasification as well as the influence of fuel ash layers on the bed material on the catalytic activity.

2. Materials and methods

2.1. DFB steam gasification fundamentals

Fig. 1 shows a simplified scheme of the DFB steam gasification process (left), as well as a sketch of the advanced 100 kW$_{th}$ pilot plant at TU Wien (right). Fuel is added to the GR, where it is gasified by steam. The char remaining after gasification is transported to the CR with the bed material. Inside the CR char combustion occurs, heating up the bed material. The hotter bed material is transferred back to the GR, providing the gasification with the heat needed for the endothermal gasification reactions.

The advanced 100 kW$_{th}$ DFB reactor system has two GRs, a lower

and an upper GR. The lower GR is a bubbling fluidised bed fluidised with steam. The upper GR has several geometrical constrictions to create turbulent zones [10,42], increasing the contact between the hot bed material coming from the CR and the gas produced in the lower GR. Gravity separators are used instead of cyclones to allow for the use of softer bed materials [25] like limestone [43,44].

2.2. Procedure of the DFB steam gasification experiments

For the heating-up procedure of the 100 kW$_{th}$ pilot plant, both reactors are operated with air. The plant is heated up electrically until 400 °C are reached. From that point on, wood pellets in the GR and heating oil in the CR are used to heat the plant further to approx. 850 °C. After this temperature is reached, the fluidization of the GR is switched to steam. Typically, the plant is operated with wood pellets until stable operation is reached. Afterwards, the experiments with the planned fuels start.

A variety of experiments were performed throughout this study. A summary of all the experiments performed, as well as their experimental time, is given in Table 1. Fuels and bed materials were chosen to cover a wide range of catalytic activity, based on the initial activity of the bed material or the ash content and composition. Two experiments were performed with SW and fresh olivine (#8 and #9) to also examine the influence of temperature on the catalytic activity (see Table 2).

2.2.1. Measurements

All relevant temperatures, pressures and flow rates were recorded continuously. The product gas composition (H_2, CO, CO_2, CH_4) was measured continuously with a Rosemount NGA2000. C_2H_4, C_2H_6, C_3H_8 and N_2 were measured every 12–15 min by a PerkinElmer ARNEL – Clarus 500 gas chromatograph. The product gas was sampled from the point indicated in Fig. 1 (right). Previous research has shown that the counter-current column atop the lower GR further increases the observed catalytic activity by increasing H_2 yields and reducing the product gas tar content [45].

Tar samples were collected discontinuously by isokinetically taking samples with impinger bottles filled with toluene to condense and dissolve all condensable hydrocarbons. The mass of tar left after vacuum evaporation of the solvent is characterised as gravimetric tar. Medium molecular weight tars were analysed by a gas chromatograph coupled with mass spectroscopy (GCMS) giving the GCMS tars. All the tar contents given exclude benzene, toluene, ethylbenzene and xylene, due to the sampling procedure. The tar dew points of the detected GCMS tar compounds were calculated with the calculation tool from ECN.TNO [46]. This is an important value regarding the fouling of downstream equipment of the gasifier. A more detailed description of the measurements performed can be found in the work by Mauerhofer et al. [47].

2.2.2. Validation of process data

The software IPSEpro was used to calculate mass and energy balances of the gasification experiments and thereby validating the measured data. For the calculations an extensive model library was used [48]. With IPSEpro it is also possible to calculate values that were not measured during the experiments.

2.3. Bed materials

K-FS, fresh and layered olivine, as well as limestone were chosen for this study to provide a range of bed materials with varying catalytic activity. The activated olivine originates from the industrial DFB steam gasification plant in Senden, near Ulm, Germany [49] and already possesses a fuel ash layer from long-term operation in a plant.
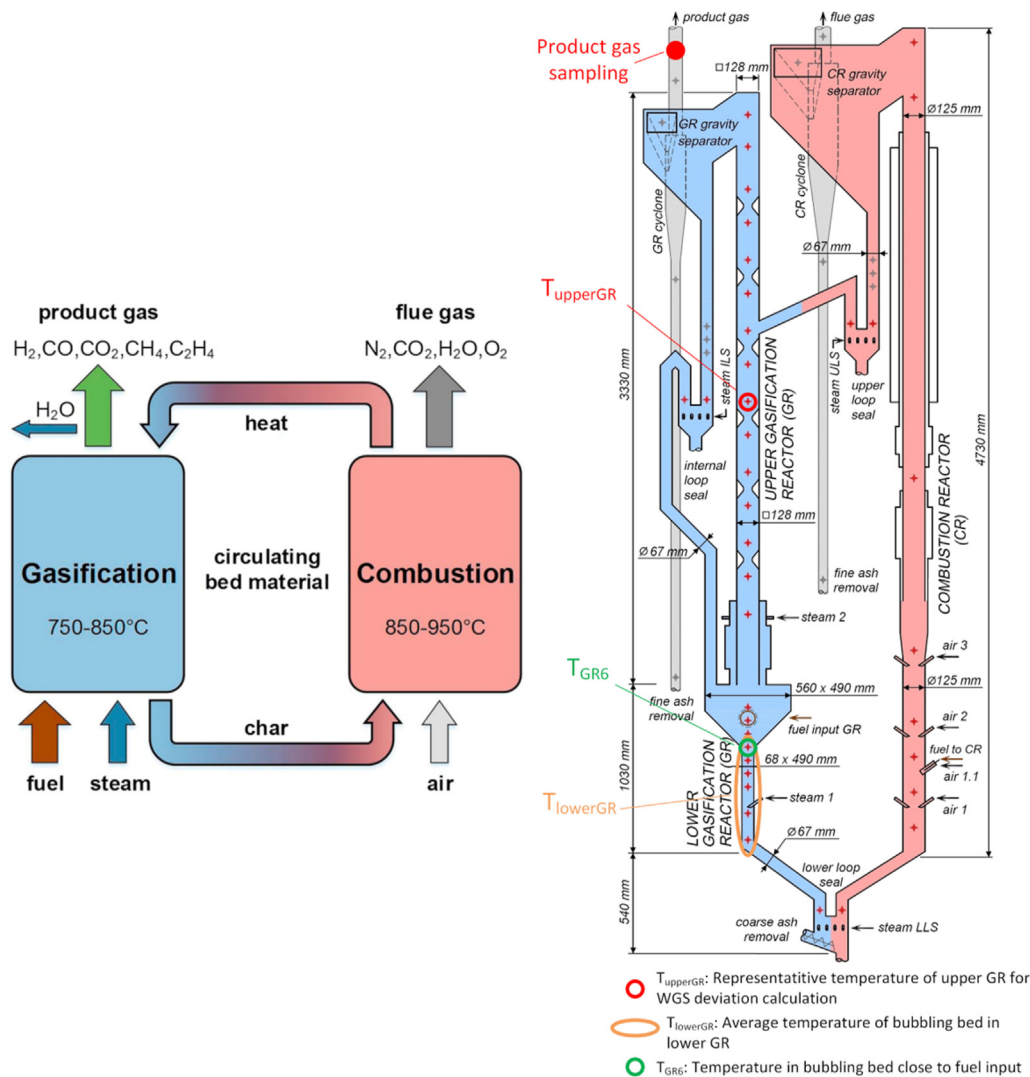
Fig. 1. Dual fluidised bed steam gasification scheme. Left: Simplified scheme of DFB steam gasification. Right: Simplified flow chart of the advanced 100 kW$_{th}$ DFB reactor system at TU Wien marked with sampling points and temperature measurement points. Adapted from Benedikt et al. [67].

Table 1
Experiments performed throughout this study as well as the experimental time they were performed.

No.	Bed material (blend) (bed material ratios are mass fractions given in %)	Fuel (blend) (fuel ratios are mass fractions given in % on a dry basis)	Experimental time in min
#1	K-FS (90) −Limestone (10)	Softwood (SW)	90
#2	K-FS (90) −Limestone (10)	Bark (70) − chicken manure (CM) (30) (B7C3)	150
#3	K-FS (90) −Limestone (10)	CM	90[a]
#4	K-FS	SW	70
#5	K-FS	Bark (59.5) − straw (15) − CM (25.5) (BSC)	160
#6	K-FS (50) −Limestone (50)	SW	210
#7	Limestone	SW	420
#8	Fresh olivine	SW	120
#9	Fresh olivine	SW	240
#10	Activated olivine	SW	150
#11	Activated olivine	B7C3	90

[a] Experiment #3 was performed consequently to experiment #2.

Olivine is currently the bed material used in commercial plants. Due to its mechanical properties it is a suitable bed material for fluidised bed applications. Compared to quartz, the bed material

mainly used in fluidised bed combustion, it has an observable catalytic activity towards gasification reactions [32]. However, the activated olivine has a non-negligible content of heavy metals, such

Table 2
Performance indicating key figures for the conducted experiments.

	Steam to Fuel Ratio (daf[a])	Steam to Carbon Ratio	Product gas yield	Steam-related H_2O conversion	Fuel-related H_2O conversion
	$kg_{steam}\ kg^{-1}_{fuel,daf}$	$kg_{H2O}\ kg^{-1}_{fuel,carbon}$	$Nm^3_{PG^b,dry}\ kg^{-1}_{fuel,dry}$	$kg_{H2O}\ kg^{-1}_{H2O}$	$kg_{H2O}\ kg^{-1}_{fuel,daf}$
#1	0.8	1.7	1.36	0.29	0.24
#2	0.8	1.6	1.44	0.34	0.26
#3	0.9	1.8	1.52	0.38	0.34
#4	0.9	1.8	1.17	0.14	0.12
#5	0.9	1.8	1.34	0.24	0.23
#6	0.8	1.5	1.44	0.33	0.26
#7	0.75	1.4	1.36	0.31	0.23
#8	0.9	1.8	1.36	0.26	0.23
#9	1	2	1.35	0.22	0.22
#10	0.85	1.7	1.46	0.31	0.27
#11	1.2	2.3	1.68	0.33	0.40

[a] daf dry ash free.
[b] PG product gas.

as nickel and chromium [20]. Due to attrition in the fluidised bed, part of the bed material, and therefore heavy metals, end up in the ash fractions. This makes further use of the accruing ash impossible and additionally leads to increased costs due to the rather costly ash disposal [20].

Limestone ($CaCO_3$) and dolomite ($CaO \cdot Mg(CO_3)_2$) are naturally occurring minerals with a significant catalytic activity if calcined prior to application or during operation [50,51]. Several researchers attribute the catalytic activity to MgO and CaO [21,32,52,53]. However, limestone and dolomite are soft minerals with a Moh's hardness of only 3 [27] and 3.5−4 [27], respectively, compared to the Moh's hardness of olivine (6.5−7 [27]) and quartz (7 [27]). The low hardness leads to a high attrition during fluidised bed operation, leading to a higher bed material demand as well as higher dust contents in the product gas [24]. Additionally, limestone has low heat transfer properties in comparison to olivine [24].

Feldspar is another mineral that is suitable as bed material. Its Moh's hardness is 6 [27]. Alkali-feldspar, a mixture of K-FS (0.48 kg kg^{-1}), Na-feldspar (Na-FS) (0.40 kg kg^{-1}), Ca-feldspar (0.06 kg kg^{-1}) and quartz (0.06 kg kg^{-1}), was used in experimental investigations to upgrade the product gas by reducing the tar content and increasing the H_2 content [54]. The same alkali-feldspar was used as bed material in the Chalmers indirect gasifier in Gothenburg, which is also based on the DFB technology. The experiments showed that, similar to olivine, an ash-rich layer formed on the bed material during operation. The long-term exposure to fuel ash led to a 59% total tar reduction compared to fresh alkali-feldspar [55]. In contrast, long-term exposure of olivine led to a maximal total tar reduction of only 30% [55]. Faust et al. [56] and Hannl et al. [57] studied alkali-feldspars extensively in a two-part study, concluding that K-FS is more stable for fluidised bed applications than Na-FS for K-rich fuels. The Na-FS reacts with the fuel potassium, thereby expelling sodium and silicon out of the particle. The increased amount of sodium and silicon for the reaction with the fuel ash might lead to the formation of ash melt and agglomerates [58,59]. Therefore, a feldspar fraction mainly consisting of K-FS (K-FS (0.87 kg kg^{-1}), Na-FS (0.07 kg kg^{-1}), quartz (0.04 kg kg^{-1}) and clay substance (0.02 kg kg^{-1}) [36]) was chosen for this study. This was done to reduce the complexity of the system and better study the effects of bed material, fuel and bed material−fuel interactions. However, pure K-FS shows no catalytic activity regarding gasification reactions [31]. Therefore, it is also a model substance for catalytically inactive bed materials.

Two mixture ratios between limestone and K-FS were applied to further understand the influence of bed material on the catalytic activity. The addition of 10−20% limestone is typically performed in the pilot plant since it was shown to have a similar effect to fuel ash

layers [10]. The mixture with 50% limestone was chosen with the aim of maximising catalytic activity while still maintaining a high heat transfer [24].

2.4. Fuels and fuel preparation

The fuels used in this study were softwood (SW), chicken manure (CM), a bark−chicken manure mixture (B7C3) and a bark−straw−chicken manure mixture (BSC). The fuel ash composition, measured by X-ray fluorescence, as well as the ash content are depicted Fig. 2. All fuels and fuel blends were either obtained as 6 mm pellets or milled and pelletised to a diameter of 6 mm (see Fig. 3).

Wood chips were used as fuel in the demonstration plant in Güssing [60]. Due to the smaller scale of the 100 kW$_{th}$ pilot plant at TU Wien, SW pellets are used as an alternative since previous tests have shown that the product gas composition is comparable [60] and the fuel dosing, can be performed more accurately. Due to the accurate fuel dosing mass and energy balances can be easily established. SW also has a comparatively low ash content (see Fig. 2), reducing the need for ash removal during long-term operation.

CM was chosen as phosphorus-rich fuel with a significant amount of ash. Some experience is available regarding the
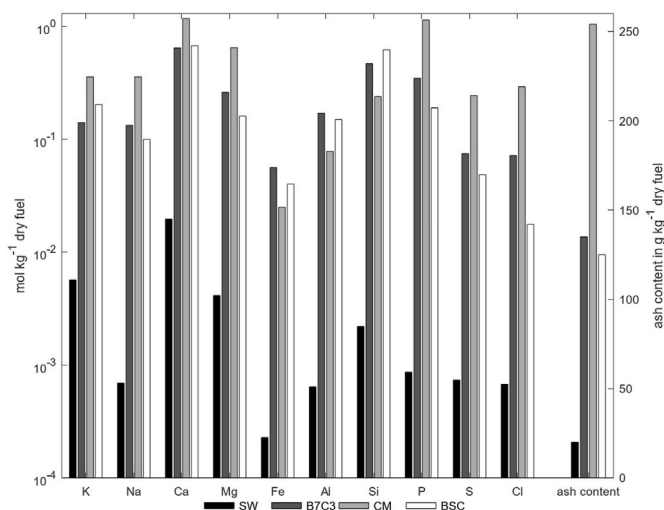

Fig. 2. Fuel ash composition determined by XRF analysis for the fuels used. The ash content of the fuels is depicted on the right side.
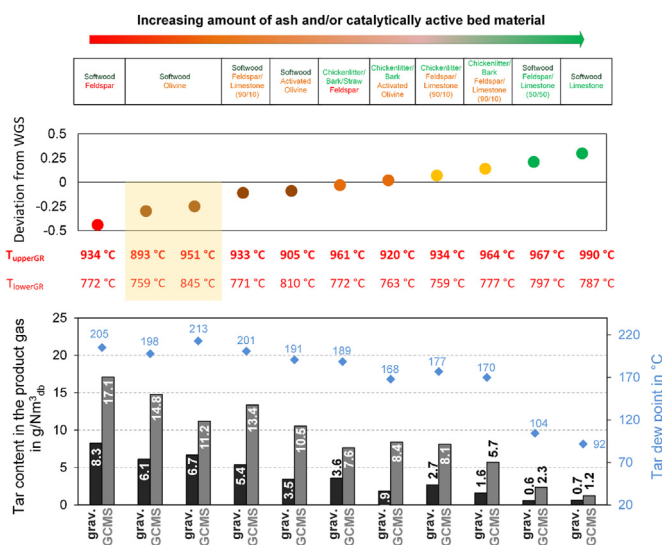
Fig. 3. Summary of the gasification experiments performed. The experiments are sorted by their deviation from the WGS equilibrium. The lower image depicts the tar content in the product gas as well as the tar dew point.

gasification of CM and poultry manure in general [61–63]. Horvat et al. postulated that the gasification of poultry litter leads to low tar contents in the product gas due to catalytically active ash-forming elements [63], though the higher contents of nitrogen in the fuel lead to higher contents of NH_3 and nitrogen-containing tar compounds [62,63].

Bark is a waste product from wood utilization and accumulates in high quantities in industries like pulp and paper. Additionally, it is a rather calcium-rich fuel. Extensive knowledge about bark gasification at industrial scale is available for the GoBiGas demonstration plant in Gothenburg [64]. More than 750 h of operation showed that a similar product gas composition can be achieved to that of wood pellets. Bark was used in the fuel mixtures opposed to softwood since it has a higher ash content. Therefore, lower additions of bark are necessary to obtain a considerable fraction of bark ash in the fuel mixture (99% of SW would be necessary to obtain the same ash fraction in the mixture).

Straw is a typical waste stream from agriculture and contains high amounts of silicon. Previous gasification experiments with straw have shown a high tendency for ash melting and agglomeration, caused by the high contents of alkali metals and silicon [29]. Straw ash has a comparatively low ash softening temperature of 830 °C (determined according to DIN 51730-A). This low ash softening temperature makes straw unsuitable for DFB steam gasification at the temperatures it is normally operated at (around 800 °C [65]). Therefore, straw was only used to a small degree throughout this study, namely as a component in the BSC fuel mixture. By only adding a small ratio of straw to the BSC fuel mixture it was possible to keep the ash softening temperature (1180 °C) in an acceptable range.

2.5. SEM/EDS measurements

The bed material sampled from gasification was gathered and fixed in epoxy resin. The samples were dry-polished to reveal the bed material cross-sections. In this way it is possible to study the layer growth and layer composition on the bed particles. A Carl Zeiss Evo LS15 scanning electron microscope (SEM) equipped with an Oxford X-Max 80 energy dispersive X-ray spectrometer (EDS) was used for elemental analysis. Area analyses were performed to

acquire the elemental distribution over the particles and particle layers. The analysed particles were chosen randomly and around 10 area analyses were performed for each sample.

2.6. Water-gas-shift reaction

The catalytic activity was quantified as the WGS equilibrium deviation. The WGS reaction is the reaction of carbon monoxide and water to carbon dioxide and hydrogen:

$$CO + H_2O \rightleftarrows CO_2 + H_2$$
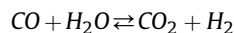
To calculate the WGS equilibrium deviation the following equation was used [18]:

$$p\delta_{eq,WGS}(p_i, T) = log_{10}\left[\frac{\prod_i p_i^{\nu_i}}{K_{P,WGS}(T)}\right]$$

$p\delta_{eq,WGS}$ gives the logarithmic WGS equilibrium deviation, dependent on the partial pressure (p_i) and temperature (T). ν_i indicates the stoichiometric factor of component i ($i=CO$, H_2O, CO_2, H_2) and $K_{p,WGS}(T)$ is the equilibrium constant of the WGS reaction at temperature T.

A negative value obtained with this equation indicates that the equilibrium of the reaction was not reached. Positive values represent too much product and a change in reaction direction. A value of zero denotes the equilibrium state. The software HSC 6 was used to obtain the necessary reaction data [66]. The WGS reaction was chosen to quantify the catalytic activity since it is an important gas phase reaction in the field of biomass gasification [9]. Additionally, no side reactions can occur and it is one of the main reactions dictating the H_2:CO ratio, which is of importance for further synthesis.

Another reaction influencing the H_2 content in the product gas is the reformation of tars:

$$C_mH_n + mH_2O \rightleftarrows mCO + \left(m + \frac{n}{2}\right)H_2$$
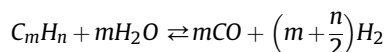
It was shown that layered bed materials, which are catalytically active for the WGS reaction, are also catalytically active regarding tar reformation [31,32]. At 800 °C, the temperature normally prevalent in the GR [65], the WGS equilibrium can only be reached with the aid of a catalyst [9], thus being a good indicator for the catalytic activity. The WGS equilibrium deviation is therefore a suitable parameter to quantify the performance of gasification regarding the product gas quality (H_2:CO ratio and tar content).

In addition to the DFB steam gasification experiments, separate isolated WGS experiments were performed with selected bed material samples to further study the influence of bed material, fuel ash and fuel ash layers on the catalytic activity during DFB steam gasification. For this purpose, experiments were performed in a micro-scale test-rig. The micro-scale test-rig consists of a quartz glass reactor (4 mm inner diameter) which is heated by a heating furnace to 850 °C. The bed material sample was placed inside the quartz glass reactor with the help of quartz wool and was filled in to a height of 5 cm. The volume was kept constant rather than the weight to overcome density differences of different samples. The goal was to mimic a fluidised bed with the same bed height, rather than a fluidised bed with the same mass, since the bed height is fixed by the dimensions of the fluidised bed reactor. Steam was provided by an evaporator mixer by Bronkhorst with nitrogen as carrier gas. The gas flows were set to 20 Nl h^{-1} CO, 16 g h^{-1} H_2O and 25 Nl h^{-1} N_2, which corresponds to a slight steam excess. The maximal H_2 and CO concentrations were observed shortly after the start of the experiment before the concentrations of H_2 and CO

rapidly decreased before reaching a stable level. To exclude initial deactivation behaviour evaluation of the gas composition was started 30 min after the maximal detected concentration. After these 30 min, an average gas composition was determined for 0.75 h.

The gas was then cooled down in a laboratory cooler to condense all the water before being measured in two EasyLine Continuous Gas Analysers by ABB (model EL3020). The measurable gas components were O_2, H_2, CO, CO_2 and CH_4.

3. Results and discussion

Fig. 4 depicts a comparison of all the gasification experiments performed and summarises performance indicating key figures. The experiments are sorted according to their WGS equilibrium deviation, starting with the most negative deviation. The upper graph shows the WGS equilibrium deviation and the lower graph shows the tar content in the product gas. The gasification experiments with the most catalytically active materials even show a positive WGS equilibrium deviation. This means that more H_2 and CO_2 were produced than the equilibrium concentration dictates. One reason for that is that the WGS reaction is only one of many reactions occurring during gasification. Steam reforming of tars is also enhanced when a catalytic increase regarding the WGS is observed, which produces additional CO and H_2. The deviation from the WGS reaction is chosen as the parameter because it allows a comparison of the H_2:CO ratio reached, while also being able to compare experiments performed at varying temperatures. The temperatures given for each experiment are the temperature in the upper GR and the lower GR as indicated in Fig. 1. The experiments were regulated to comparable lower GR temperatures at around 770 °C. Experiments #6, #7, #9 and #10 were taken from previous studies (mostly reported in Ref. [24]) to supplement the available data though they were performed at different temperatures.

The upper GR temperature was used to calculate the WGS equilibrium deviation since it is closer to the product gas sampling point. The temperatures observed in the upper GR varied between 900 and 1000 °C. Due to the different heat capacities of the bed materials, different temperatures are observed in the upper GR. Overall, an increase of the WGS reaction also led to a decrease of both the gravimetric and GCMS tar content. It was shown that catalytic bed materials are active both for the WGS reaction and for tar reforming [32]. A wide range of tar contents could be observed during the experiments. The gasification with pure limestone as the bed material led to a reduction to a tenth of both the GCMS and gravimetric tar contents of the least catalytically active experiment with K-FS and SW. Apart from the reduction in tar content a reduction in the tar dew point was also detected. A tar dew point below 180 °C enables the possibility of dry cleaning (i.e. fabric filter) of the product gas [24] and reduces the risk of fouling of downstream equipment.

It can be seen that both the bed material and the fuel have an impact on the WGS equilibrium deviation.

Focusing on the experiments using SW as fuel, it can be seen, that the catalytic activity of the bed materials behaves as expected. K-FS, a known inactive bed material [31,35], shows the most negative deviation in this study. Fresh olivine has a slightly less negative WGS equilibrium deviation, with activated olivine having an even less negative deviation. A comparable catalytic activity can be observed for the 90/10 mixture of K-FS and limestone. Even higher admixtures of limestone (50/50) already led to a positive WGS equilibrium deviation. The gasification with pure limestone led to the most positive WGS equilibrium deviation.

Comparing experiments with the same bed material but different fuels always shows that the experiments with SW have the most negative deviation compared to the experiments with other fuels. This is especially clear for K-FS but can also be seen for K-FS (90)/Limestone (10) and activated olivine.

The two experiments with olivine and SW at different temperatures show the subordinate role of gasification temperature on the WGS equilibrium deviation. Though, an impact of gasification temperature on product gas tar content can clearly be seen.

Carbon mass balances over the gasification reactor (see Fig. 4) are depicted for the experiments of SW gasified with K-FS, limestone and activated olivine as bed materials, covering a wide range of catalytic activity. Most of the carbon introduced with the fuel can be found in the product gas. Due to clarity the gaseous part of the product gas is shown as a whole and not subdivided into its compounds. The definite gas fractions are summarised in Table A- 1, comparing measured and validated values.

It can also be seen that the catalytic activity has a subordinate role regarding the amount of char transported to the combustion reactor. The amount of char mainly influences the temperature in the system, as higher temperatures are maintained when more char is burned in the combustion reactor.

3.1. In-situ activation during gasification

The effect of fuel ash on the catalytic activity during DFB steam gasification can be best seen in the experiment with BSC. Fig. 5 depicts the temperature profile, as well as the product gas composition, for the experiments with SW and BSC, both with K-FS as bed material. T_{GR6} is depicted instead of $T_{lowerGR}$ since this temperature measurement is especially sensible to process fluctuations therefore being a first indicator for problems during operation. The experiment with SW was performed for 70 min, reaching a steady-state operation in the last 30 min. For clarity only these last 30 min are depicted in Fig. 5. During steady-state operation the temperature and the gas composition remained constant, with a slight reduction in C_2H_4 content observed. These last 30 min
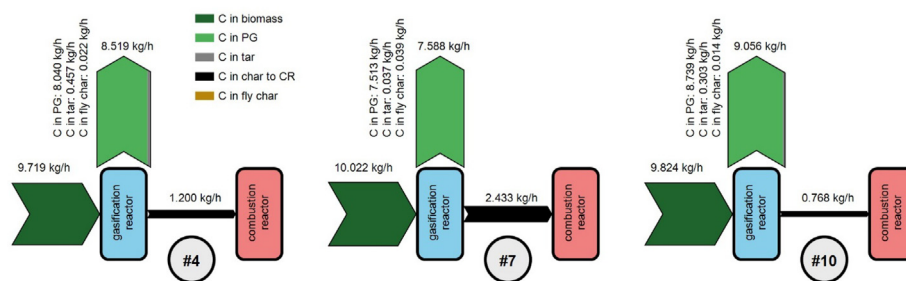

Fig. 4. Carbon mass balance over the gasification reactor for experiments #4, #7 and #10. Most of the carbon fed to the reactor via the fuel can be found in product gas (PG). Another relevant amount can be found in the char being transported to the combustion reactor (CR).
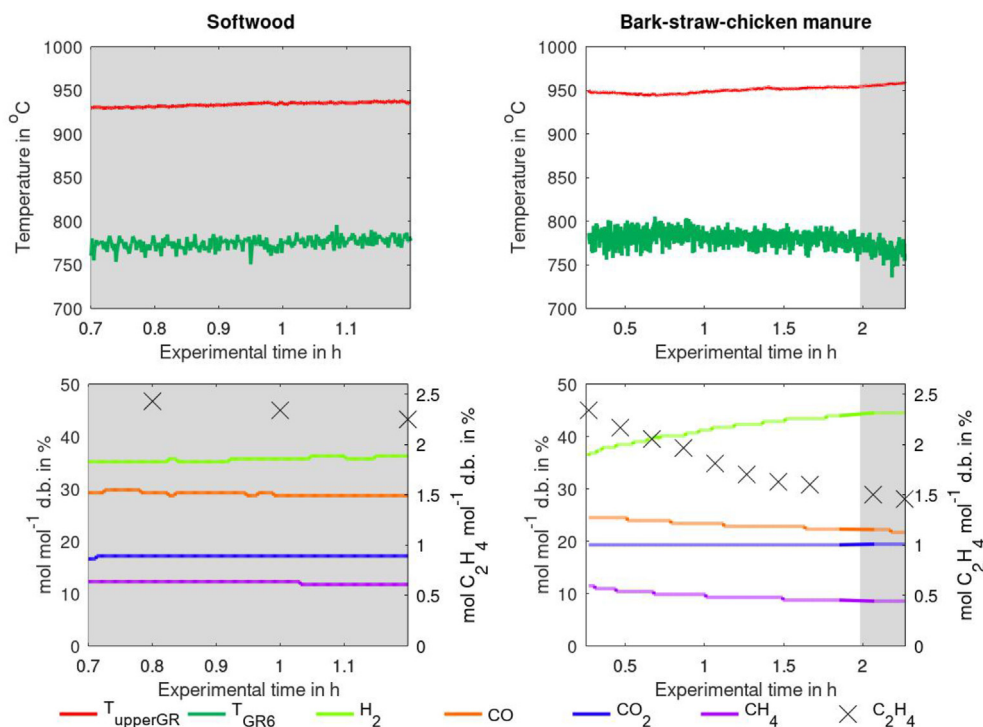
Fig. 5. Comparison between operation with SW and BSC with K-FS as bed material. C_2H_4 was only measured discontinuously. The grey-shaded areas in the graphs indicate the measurement intervals used for the calculations of the WGS deviation depicted in Fig. 4.

(indicated in grey in Fig. 5) were also used to determine the deviation from the WGS equilibrium in Fig. 4.

Stable operation (meaning a constant temperature in the GR) was also achieved for BSC. The product gas composition, on the other hand, changed during this time. The increase in H_2 and decrease of CO can be linked to an increase of the WGS reaction. The increase in catalytic activity can be explained by the accumulation of fuel ash in the system. Due to the high ash content of the fuel (see Fig. 2) ash accumulates at a faster rate than for e.g. SW. Due to the low initial catalytic activity of K-FS, the effect of fuel ash was easily observable. This significant change in the product gas composition described in this study was for the first time ever observed in the 100 kW_{th} pilot plant in this scale, though a change in product gas composition was occasionally observed previously but never in a scale worth reporting.

During the experiment with BSC an increase of the volume flow up to 30% was measured. Because of this, the observed decrease in CH_4 can be linked to a dilution effect and not to a decreased ratio of production, as was already established [67]. The increase in dry gas volume flow is caused by an increased occurrence of tar reforming and therefore lower tar contents in the product gas. This can be explained by the fact that a higher occurrence of the lower deviation from the WGS reaction also leads to lower tar content [31,67]. C_2H_4, an indicator for the tar content [67], also decreased during the experiment.

The gasifier was operated with BSC for 160 min before complications led to a shutdown of the GR. Temperature fluctuations in the lower part of the reactor occurred, which are usually an indication of problems regarding the intermixing of the bed. This might be explained by the comparatively high ash contents of the BSC fuel compared to the relatively ash-free SW. In the case of fluctuating temperatures, the plant has to be shut down immediately to prevent any damage to the equipment. To be able to better handle fuels with high ash contents, adaptations of the ash removal system

would be necessary. The test plant currently has no continuously operated bed ash removal, since it is designed for short-term operation.

3.2. Initial layer formation

Fig. 6 shows EDS mappings for several experiments. The short operation time of the 100 kW pilot plant led to the development of
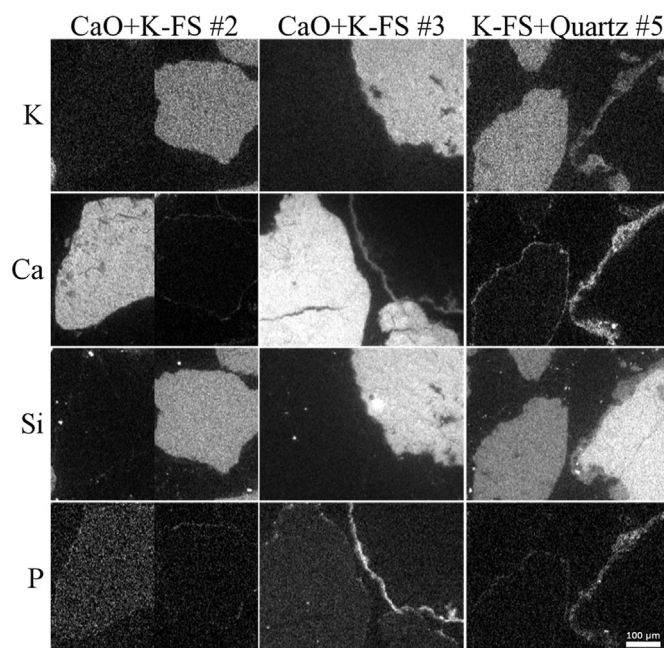

Fig. 6. EDS mappings for selected bed material samples.

only an initial layer, with layers too thin for quantitative analysis. Exemplary EDS mappings are presented for experiments #2 (B7C3 + K-FS/Limestone 90/10), #3 (CM + K-FS/Limestone 90/10) and #5 (BSC + K-FS). Olivine was omitted from this work since various publications are already available covering olivine layer formation and characterization [33,68−73].

The brightness in an EDS mapping gives the concentration of a specific element; brighter areas contain higher concentrations of the respective element while darker areas show lower concentrations. With the brightness alone, it is not possible to derive the concentration, since the brightness only gives the relation for a specific mapping and is different for every mapping and element. For clarity, only the most relevant elements are depicted in Fig. 6, namely potassium, calcium, silicon and phosphorus.

K-FS particles are depicted for experiments #2, #3 and #5. K-FS consists of potassium, silicon and aluminium (not depicted in Fig. 6). Initial layer formation can be detected for all K-FS particles. Layers on K-FS are characterised by calcium and phosphorus. Layers of different thickness formed on the K-FS particles. Layers of comparable thickness formed during experiments #2 and #5 with slightly more pronounced layers forming during experiment #5. The similarity in layer thickness can be explained by both the comparable operational time (150 vs. 160 min, see Table 1) and a similar ash content (see Fig. 2). Thicker layers formed during experiment #3. This experiment was performed consecutively to experiment #2, explaining the increased layer thickness.

Limestone particles can be seen for experiments #2 and #3 and can be distinguished by the high concentration of calcium. No layer formation can be detected for limestone. The low abrasion resistance of limestone might be the reason why no layer formation could be observed. A quartz particle, which is a common impurity in K-FS bed material, was also detected for experiment #5. Quartz particles are characterised by high silicon concentrations. A layer rich in potassium, calcium and phosphorus formed on these quartz particles. It can additionally be seen that the layer formed on the quartz particle is thicker than the layer formed on K-FS [37].

Fuel ash layers are linked to an increase in catalytic activity during DFB steam gasification [34]. This can be seen in this work when comparing the WGS equilibrium deviation for fresh and layered olivine though most differences observed for the different experiments in this work were caused by the fuel ash directly and not by layer formation. Even though initial layer formation can be observed (see Fig. 6), the effect of these initial layers is negligible since no change in product gas composition could be observed during the operation of ash-rich fuels. The only exception is the experiment with K-FS as bed material and BSC as fuel. The effect of layer formation is easily observed during this experiment since the initial catalytic activity of the bed material is so low. Since all the other experiments with ash-rich fuels contain at least some ratio of catalytically active bed materials (limestone, olivine and layered olivine), the effect of the fuel ash is less pronounced in the time-scale of the experiments.

3.3. Isolated WGS experiments

Selected bed material samples were further studied in isolated WGS experiments to further study the influences on the WGS reaction. Fig. 7 depicts the results obtained for these experiments sorted according to decreasing WGS equilibrium deviation. The experiments were not only performed with samples from various gasification test runs, but also with fresh bed materials and layered olivine, before it was used in the 100 kW$_{th}$ pilot plant. It has to be noted, that these experiments were designed to lead to conversions that deviated greatly from the equilibrium to be able to better quantify the potential of different bed materials. The samples used
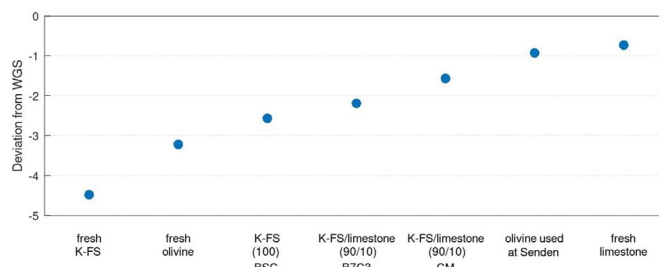

Fig. 7. WGS equilibrium deviation determined in isolated WGS experiments.

for these experiments were bottom ash samples which mainly contain the bed material and bigger ash particles, while smaller ash particles are collected as fly ash from the cyclone. During the gasification in the 100 kW$_{th}$ pilot plant, both the bed material and the smaller ash particles are in contact with the developing product gas, and therefore contribute to the catalytic activity. In these isolated experiments, special focus was given to the bed material as well as the bed material layers.

The experiments with the unused bed materials can be compared to the experiments with SW, since SW has nearly no ash content that could have an impact on the catalytic activity. Overall, a similar trend regarding the WGS equilibrium deviation can be observed as during the gasification experiments shown in Fig. 4. The results of these experiments further support that the WGS reaction is one of the main reactions occurring during gasification.

Only layered olivine is considerably more active during the isolated WGS experiments compared to its activity during gasification in the 100 kW$_{th}$ pilot plant. This might be explained by the fact that during gasification the fuel ash actually dilutes the catalytic activity of the already layered bed material. The strong impact of the fuel ash in the system is further supported by the changing gas composition observed during the gasification of BSC with pure K-FS as bed material. The effect of smaller particles might also be one reason for the high catalytic activity of limestone observed during gasification. Since limestone is a comparatively soft bed material the content of smaller particles (produced by attrition) is increased, further supporting the importance of ash and bed material dust for the catalytic activity. Another explanation for the considerably higher catalytic activity observed for layered olivine in these isolated experiments might be that CaO and calcium-rich fuel ash layers are more catalytically active regarding the WGS reaction compared to other reactions occurring during gasification. The sequence shown in Fig. 7 can also be obtained when sorting according to the calcium content on the bed particle surfaces. K-FS and fresh olivine contain no calcium and are followed by the layered K-FS from BSC gasification. The substitution of 10% of K-FS by limestone considerably increased the amount of surface-available calcium, leading to the observed decrease in WGS deviation. The slightly lower deviation for CM originates from the fact that this gasification experiment was performed directly after the gasification run with B7C3, leading to slightly thicker layers, and more enrichment of calcium on the bed material surface can be assumed. The layered olivine exhibits a fully developed layer with considerable calcium content and the highest calcium content is observed for pure limestone.

To summarise, the experiments performed show that there is a variety of different options to change the catalytic activity during DFB steam gasification. The addition of limestone is currently performed on an industrial scale during start-up until the desired catalytic activity is achieved by layer formation [74]. The use of ash-rich fuels might make it possible to omit the use of limestone

entirely. Further research into the role of both the bed material and fuel ash on different reactions during gasification is necessary before this step. The exclusive use of limestone as bed material was performed in the pilot plant with a smooth gas−solid separation system and did not show negative effects on operation [25], but has to be validated in the long-term operation of commercial plants.

4. Conclusion

A variety of experiments were performed at a 100 kW$_{th}$ DFB steam gasification pilot plant. Arranging the experiments by their WGS equilibrium deviation showed that both the bed material and the fuel ash can have an impact on the catalytic activity. The lowest catalytic activity was observed for experiments with pure K-FS and olivine. The low initial catalytic activity of K-FS made it possible to observe initial activation with the ash-rich BSC fuel. Increasing the amount of limestone significantly decreased the negative WGS equilibrium deviation. High amounts of limestone even lead to a positive WGS equilibrium deviation by catalysing reactions apart from the WGS reaction. The results showed that a variety of options are available to increase the catalytic activity during DFB steam gasification. Comparisons at different gasification temperatures did not show a significant impact of temperature on the WGS deviation. Nevertheless, an influence on the tar content could be observed. The interaction between different parameters, such as temperature and the addition of catalytically active materials, has yet to be studied in more detail to gain deeper understanding of the underlying mechanisms. Also, further research is necessary to be able to exploit the knowledge reported in this study and deliberately change the product gas composition in a desired way.

EDS mappings showed initial layer formation for a range of experiments with layers most often enriched in calcium, potassium and, if available from the fuel, phosphorus. Long-term experiments will be necessary to develop thicker layers to be able to quantify the layer composition on the bed material particles. Long-term experiments might also prove whether layer formation is possible on limestone or if the attrition resistance of limestone is too low for layers to form on it.

Isolated WGS experiments showed a similar order of catalytic activity for the studied samples. This shows that the WGS reaction is one of the main reactions influencing the product gas composition. Further experiments are necessary to further understand the role of the WGS reaction as a characterization for the catalytic activity during gasification. Especially the influence on the product gas tar content is of importance, since tar measurements are typically not performed continuously.

Credit author statement

Katharina Fürsatz: Conceptualization, Methodology, Formal analysis, Investigation, Writing − original draft, Visualization, Project administration. Josef Fuchs: Conceptualization, Methodology, Validation, Investigation, Writing − review & editing, Visualization. Florian Benedikt: Validation, Investigation, Writing − review & editing. Matthias Kuba: Resources, Writing − review & editing, Supervision, Funding acquisition. Hermann Hofbauer: Resources, Writing − review & editing, Supervision, Funding acquisition.

Declaration of competing interest

The authors declare that they have no known competing financial interests or personal relationships that could have appeared to influence the work reported in this paper.

Appendix

Table A1
Comparison of the measured product gas composition and the data validated with IPSEpro.

			H$_2$	CO	CO$_2$	CH$_4$	C$_2$H$_4$	H$_2$O
#1	Measured	vol%$_{db}$[a]	39.6	23.1	19.7	11.1	2.1	39
	Validated in IPSEpro	vol%$_{db}$	38.9	25.1	20.8	11.8	2.0	35
#2	Measured	vol%$_{db}$	43.8	23.5	19.9	8.0	1.1	31
	Validated in IPSEpro	vol%$_{db}$	43.8	23.5	19.9	8.0	1.1	31
#3	Measured	vol%$_{db}$	43.3	20.7	20.4	8.7	2.2	35
	Validated in IPSEpro	vol%$_{db}$	40.1	21.0	19.8	8.4	2.1	31
#4	Measured	vol%$_{db}$	35.6	29.1	17.1	12.1	2.3	46
	Validated in IPSEpro	vol%$_{db}$	35.7	29.9	17.8	12.8	2.3	45
#5	Measured	vol%$_{db}$	44.3	21.9	19.3	8.7	1.5	40
	Validated in IPSEpro	vol%$_{db}$	44.2	22.3	20.0	8.4	1.5	40
#6	Measured	vol%$_{db}$	45.6	20.2	19.5	8.6	0.6	31
	Validated in IPSEpro	vol%$_{db}$	45.8	21.5	20.9	9.1	0.7	31
#7	Measured	vol%$_{db}$	47.3	20.6	22.1	8.5	0.5	31
	Validated in IPSEpro	vol%$_{db}$	47.4	21.3	21.2	8.9	0.5	31
#8	Measured	vol%$_{db}$	36.0	25.8	19.6	11.7	2.5	41
	Validated in IPSEpro	vol%$_{db}$	39.1	25.9	19.8	11.4	2.5	38
#9	Measured	vol%$_{db}$	39.0	26.7	18.7	9.9	1.7	43
	Validated in IPSEpro	vol%$_{db}$	39.8	27.1	18.7	10.7	1.7	42
#10	Measured	vol%$_{db}$	39.0	21.3	20.4	9.7	2.2	38
	Validated in IPSEpro	vol%$_{db}$	39.0	21.3	20.9	9.8	2.2	33
#11	Measured	vol%$_{db}$	44.8	17.2	21.6	7.6	1.6	43
	Validated in IPSEpro	vol%$_{db}$	44.8	17.5	22.1	7.6	1.6	38

[a] db dry basis.

References

[1] Meng X, de Jong W, Fu N, Verkooijen AHM. Biomass gasification in a 100 kWth steam-oxygen blown circulating fluidized bed gasifier: effects of operational conditions on product gas distribution and tar formation. Biomass Bioenergy 2011;35:2910−24. https://doi.org/10.1016/j.biombioe.2011.03.028.

[2] Hervy M, Remy D, Dufour A, Mauviel G. Air-blown gasification of Solid Recovered Fuels (SRFs) in lab-scale bubbling fluidized-bed: influence of the operating conditions and of the SRF composition. Energy Convers Manag 2019;181:584−92. https://doi.org/10.1016/j.enconman.2018.12.052.

[3] Kraussler M, Binder M, Hofbauer H. 2250-h long term operation of a water gas shift pilot plant processing tar-rich product gas from an industrial scale dual fluidized bed biomass steam gasification plant. Int J Hydrogen Energy 2016;41:6247−58. https://doi.org/10.1016/j.ijhydene.2016.02.137.

[4] Gruber H, Groß P, Rauch R, Reichhold A, Zweiler R, Aichernig C, et al. Fischer-Tropsch products from biomass-derived syngas and renewable hydrogen. Biomass Conv Bioref 2019. https://doi.org/10.1007/s13399-019-00459-5.

[5] Kraussler M, Pontzen F, Müller-Hagedorn M, Nenning L, Luisser M, Hofbauer H. Techno-economic assessment of biomass-based natural gas substitutes against the background of the EU 2018 renewable energy directive. Biomass Conv Bioref 2018;8:935−44. https://doi.org/10.1007/s13399-018-0333-7.

[6] Van der Meijden CM, Veringa HJ, Rabou LPLM. The production of synthetic natural gas (SNG): a comparison of three wood gasification systems for energy balance and overall efficiency. Biomass Bioenergy 2010;34:302−11. https://doi.org/10.1016/j.biombioe.2009.11.001.

[7] Christensen JM, Mortensen PM, Trane R, Jensen PA, Jensen AD. Effects of H2S and process conditions in the synthesis of mixed alcohols from syngas over alkali promoted cobalt-molybdenum sulfide. Appl Catal Gen 2009;366:29−43. https://doi.org/10.1016/j.apcata.2009.06.034.

[8] Binder M, Rauch R, Koch M, Summers M, Aichernig C, Hofbauer H. Influence of sulfur components on the catalytic mixed alcohol synthesis based on wood gas derived from biomass steam gasification. ETA-Florence Renewable Energies; 2017. https://doi.org/10.5071/25theubce2017-3bv.3.14.

[9] Basu P. Biomass gasification and pyrolysis: practical design and theory. Burlington, MA: Academic Press; 2010.

[10] Schmid JC, Benedikt F, Fuchs J, Mauerhofer AM, Müller S, Hofbauer H. Syngas for biorefineries from thermochemical gasification of lignocellulosic fuels and residues—5 years' experience with an advanced dual fluidized bed gasifier design. Biomass Conv Bioref; 2019. https://doi.org/10.1007/s13399-019-00486-2.

[11] Izaharuddin AN, Paul MC, Yoshikawa K, Theppitak S, Dai X. Comprehensive kinetic modeling study of CO_2 gasification of char derived from food waste. Energy Fuels 2020;34:1883−95. https://doi.org/10.1021/acs.energyfuels.9b03937.

[12] Hungwe D, Khushbouy R, Ullah S, Lu D, Yoshikawa K, Takahashi F. Effect of tire-char ash on the extent of synergy during CO2 cogasification with hydrochar from potassium-rich coconut fiber. Energy Fuels 2020. https://doi.org/10.1021/acs.energyfuels.0c00895.

[13] Latifi M, Berruti F, Briens C. Jiggle bed reactor for testing catalytic activity of olivine in bio-oil gasification. Powder Technol 2017;316:400−9. https://doi.org/10.1016/j.powtec.2016.11.057.

[14] Burra KG, Gupta AK. Role of catalyst in solid biomass gasification. American Society of Mechanical Engineers Digital Collection; 2016. https://doi.org/10.1115/POWER2016-59039.

[15] Lu Y, Jin H, Zhang R. Evaluation of stability and catalytic activity of Ni catalysts for hydrogen production by biomass gasification in supercritical water. Carbon Resources Conversion 2019;2:95−101. https://doi.org/10.1016/j.crcon.2019.03.001.

[16] Umeda K, Nakamura S, Lu D, Yoshikawa K. Biomass gasification employing low-temperature carbonization pretreatment for tar reduction. Biomass Bioenergy 2019;126:142−9. https://doi.org/10.1016/j.biombioe.2019.05.002.

[17] Lahijani P, Zainal ZA, Mohammadi M, Mohamed AR. Conversion of the greenhouse gas CO2 to the fuel gas CO via the Boudouard reaction: a review. Renew Sustain Energy Rev 2015;41:615−32. https://doi.org/10.1016/j.rser.2014.08.034.

[18] Fuchs J, Schmid JC, Müller S, Mauerhofer AM, Benedikt F, Hofbauer H. The impact of gasification temperature on the process characteristics of sorption enhanced reforming of biomass. Biomass Conv Bioref; 2019. https://doi.org/10.1007/s13399-019-00439-9.

[19] Rahbari A, Venkataraman MB, Pye J. Energy and exergy analysis of concentrated solar supercritical water gasification of algal biomass. Appl Energy 2018;228:1669−82. https://doi.org/10.1016/j.apenergy.2018.07.002.

[20] Kuba M, He H, Kirnbauer F, Skoglund N, Boström D, Öhman M, et al. Thermal stability of bed particle layers on naturally occurring minerals from dual fluid bed gasification of woody biomass. Energy Fuels 2016;30:8277−85. https://doi.org/10.1021/acs.energyfuels.6b01523.

[21] Hervy M, Olcese R, Bettahar MM, Mallet M, Renard A, Maldonado L, et al. Evolution of dolomite composition and reactivity during biomass gasification. Appl Catal Gen 2019;572:97−106. https://doi.org/10.1016/j.apcata.2018.12.014.

[22] Zhou C, Rosén C, Engvall K. Fragmentation of dolomite bed material at elevated temperature in the presence of H2O & CO2: implications for fluidized bed gasification. Fuel 2020;260:116340. https://doi.org/10.1016/j.fuel.2019.116340.

[23] Zhou C, Rosén C, Engvall K. Biomass oxygen/steam gasification in a pressurized bubbling fluidized bed: agglomeration behavior. Appl Energy 2016;172:230−50. https://doi.org/10.1016/j.apenergy.2016.03.106.

[24] Mauerhofer AM, Benedikt F, Schmid JC, Fuchs J, Müller S, Hofbauer H. Influence of different bed material mixtures on dual fluidized bed steam gasification. Energy 2018;157:957−68. https://doi.org/10.1016/j.energy.2018.05.158.

[25] Benedikt F, Fuchs J, Schmid JC, Müller S, Hofbauer H. Advanced dual fluidized bed steam gasification of wood and lignite with calcite as bed material. Kor J Chem Eng 2017;34:2548−58. https://doi.org/10.1007/s11814-017-0141-y.

[26] Vuthaluru HB, Zhang D. Effect of Ca- and Mg-bearing minerals on particle agglomeration defluidisation during fluidised-bed combustion of a South Australian lignite. Fuel Process Technol 2001;69:13−27. https://doi.org/10.1016/S0378-3820(00)00129-6.

[27] Markl G, Marks M. Minerale und Gesteine: mineralogie - Petrologie - geochemie. 3. Aufl. Berlin: Springer Spektrum; 2015.

[28] Berdugo Vilches T, Marinkovic J, Seemann M, Thunman H. Comparing active bed materials in a dual fluidized bed biomass gasifier: olivine, bauxite, quartz-sand, and ilmenite. Energy Fuels 2016;30:4848−57. https://doi.org/10.1021/acs.energyfuels.6b00327.

[29] He Z, Lane DJ, Saw WL, van Eyk PJ, Nathan GJ, Ashman PJ. Ash−bed material interaction during the combustion and steam gasification of Australian

agricultural residues. Energy Fuels 2018;32:4278−90. https://doi.org/10.1021/acs.energyfuels.7b03129.

[30] Wagner K, Häggström G, Mauerhofer AM, Kuba M, Skoglund N, Öhman M, et al. Layer formation on K-feldspar in fluidized bed combustion and gasification of bark and chicken manure. Biomass Bioenergy 2019;127:105251. https://doi.org/10.1016/j.biombioe.2019.05.020.

[31] Kuba M, Kirnbauer F, Hofbauer H. Influence of coated olivine on the conversion of intermediate products from decomposition of biomass tars during gasification. Biomass Conv Bioref 2017;7:11−21. https://doi.org/10.1007/s13399-016-0204-z.

[32] Kuba M, Havlik F, Kirnbauer F, Hofbauer H. Influence of bed material coatings on the water-gas-shift reaction and steam reforming of toluene as tar model compound of biomass gasification. Biomass Bioenergy 2016;89:40−9. https://doi.org/10.1016/j.biombioe.2015.11.029.

[33] Kuba M, He H, Kirnbauer F, Skoglund N, Boström D, Öhman M, et al. Mechanism of layer formation on olivine bed particles in industrial-scale dual fluid bed gasification of wood. Energy Fuels 2016;30:7410−8. https://doi.org/10.1021/acs.energyfuels.6b01522.

[34] Kirnbauer F, Wilk V, Kitzler H, Kern S, Hofbauer H. The positive effects of bed material coating on tar reduction in a dual fluidized bed gasifier. Fuel 2012;95:553−62. https://doi.org/10.1016/j.fuel.2011.10.066.

[35] Wagner K, Hammerl C, Kuba M, Hofbauer H. Time-dependent catalytic activation of inactive K-feldspar by layer formation during fluidized bed conversion with residual fuels. European Biomass Conference and Exhibition Proceedings; 2019. https://doi.org/10.5071/27thEUBCE2019-2CV.2.4.

[36] Fürsatz K, Kuba M, Janisch D, Aziaba K, Hammerl C, Chlebda D, et al. Impact of residual fuel ash layers on the catalytic activation of K-feldspar regarding the water−gas shift reaction. Biomass Conv Bioref 2020. https://doi.org/10.1007/s13399-020-00645-w.

[37] Wagner K, Häggström G, Skoglund N, Priscak J, Kuba M, Öhman M, et al. Layer formation mechanism of K-feldspar in bubbling fluidized bed combustion of phosphorus-lean and phosphorus-rich residual biomass. Appl Energy 2019;248:545−54. https://doi.org/10.1016/j.apenergy.2019.04.112.

[38] Häggström G, Fürsatz K, Kuba M, Skoglund N, Öhman M. Fate of phosphorus in fluidized bed cocombustion of chicken litter with wheat straw and bark residues. Energy Fuels 2020;34:1822−9. https://doi.org/10.1021/acs.energyfuels.9b03652.

[39] Yao X, Hu Y, Ge J, Ma X, Mao J, Sun L, et al. A comprehensive study on influence of operating parameters on agglomeration of ashes during biomass gasification in a laboratory-scale gasification system. Fuel 2020;276:118083. https://doi.org/10.1016/j.fuel.2020.118083.

[40] Valin S, Ravel S, Pons de Vincent P, Thiery S, Miller H, Defoort F, et al. Fluidised bed gasification of diverse biomass feedstocks and blends—an overall performance study. Energies 2020;13:3706. https://doi.org/10.3390/en13143706.

[41] Priscak J, Fürsatz K, Kuba M, Skoglund N, Benedikt F, Hofbauer H. Investigation of the formation of coherent ash residues during fluidized bed gasification of wheat straw lignin. Energies 2020;13:3935. https://doi.org/10.3390/en13153935.

[42] Schmid JC. Development of a novel dual fluidized bed gasification system for increased fuel flexibility. PhD Thesis. TU Wien; 2014.

[43] Fuchs J, Schmid JC, Müller S, Hofbauer H. Dual fluidized bed gasification of biomass with selective carbon dioxide removal and limestone as bed material: a review. Renew Sustain Energy Rev 2019;107:212−31. https://doi.org/10.1016/j.rser.2019.03.013.

[44] Fuchs J, Müller S, Schmid JC, Hofbauer H. A kinetic model of carbonation and calcination of limestone for sorption enhanced reforming of biomass. International Journal of Greenhouse Gas Control 2019;90:102787. https://doi.org/10.1016/j.ijggc.2019.102787.

[45] Mauerhofer AM, Schmid JC, Benedikt F, Fuchs J, Müller S, Hofbauer H. Dual fluidized bed steam gasification: change of product gas quality along the reactor height. Energy 2019;173:1256−72. https://doi.org/10.1016/j.energy.2019.02.025.

[46] Energy Research Center of The Netherlands (ECN. TNO) n.d. http://www.thersites.nl/completemodel.aspx. [Accessed 12 July 2019].

[47] Mauerhofer AM, Fuchs J, Müller S, Benedikt F, Schmid JC, Hofbauer H. CO2 gasification in a dual fluidized bed reactor system: impact on the product gas composition. Fuel 2019;253:1605−16. https://doi.org/10.1016/j.fuel.2019.04.168.

[48] Müller S, Fuchs J, Schmid JC, Benedikt F, Hofbauer H. Experimental development of sorption enhanced reforming by the use of an advanced gasification test plant. Int J Hydrogen Energy 2017;42:29694−707. https://doi.org/10.1016/j.ijhydene.2017.10.119.

[49] Kuba M, He H, Kirnbauer F, Boström D, Öhman M, Hofbauer H. Deposit build-up and ash behavior in dual fluid bed steam gasification of logging residues in an industrial power plant. Fuel Process Technol 2015;139:33−41. https://doi.org/10.1016/j.fuproc.2015.08.017.

[50] Soomro A, Chen S, Ma S, Xiang W. Catalytic activities of nickel, dolomite, and olivine for tar removal and H2-enriched gas production in biomass gasification process. Energy Environ 2018;29:839−67. https://doi.org/10.1177/0958305X18767848.

[51] Gusta E, Dalai AK, Uddin MdA, Sasaoka E. Catalytic decomposition of biomass tars with dolomites. Energy Fuels 2009;23:2264−72. https://doi.org/10.1021/ef8009958.

[52] Huang B-S, Chen H-Y, Chuang K-H, Yang R-X, Wey M-Y. Hydrogen production by biomass gasification in a fluidized-bed reactor promoted by an Fe/CaO

catalyst. Int J Hydrogen Energy 2012;37:6511–8. https://doi.org/10.1016/j.ijhydene.2012.01.071.

[53] Yin F, Tremain P, Yu J, Doroodchi E, Moghtaderi B. An experimental investigation of the catalytic activity of natural calcium-rich minerals and a novel dual-supported CaO-Ca12Al14O33/Al2O3 catalyst for biotar steam reforming. Energy Fuels 2018;32:4269–77. https://doi.org/10.1021/acs.energyfuels.7b03201.

[54] Berguerand N, Marinkovic J, Berdugo Vilches T, Thunman H. Use of alkali-feldspar as bed material for upgrading a biomass-derived producer gas from a gasifier. Chem Eng J 2016;295:80–91. https://doi.org/10.1016/j.cej.2016.02.060.

[55] Berguerand N, Berdugo Vilches T. Alkali-feldspar as a catalyst for biomass gasification in a 2-MW indirect gasifier. Energy Fuels 2017;31:1583–92. https://doi.org/10.1021/acs.energyfuels.6b02312.

[56] Faust R, Hannl TK, Vilches TB, Kuba M, Öhman M, Seemann M, et al. layer formation on feldspar bed particles during indirect gasification of wood. 1. K-feldspar. Energy Fuels 2019;33:7321–32. https://doi.org/10.1021/acs.energyfuels.9b01291.

[57] Hannl TK, Faust R, Kuba M, Knutsson P, Berdugo Vilches T, Seemann M, et al. layer formation on feldspar bed particles during indirect gasification of wood. 2. Na-feldspar. Energy Fuels 2019;33:7333–46. https://doi.org/10.1021/acs.energyfuels.9b01292.

[58] Davidsson KO, Åmand L-E, Steenari B-M, Elled A-L, Eskilsson D, Leckner B. Countermeasures against alkali-related problems during combustion of biomass in a circulating fluidized bed boiler. Chem Eng Sci 2008;63:5314–29. https://doi.org/10.1016/j.ces.2008.07.012.

[59] Boström D, Skoglund N, Grimm A, Boman C, Öhman M, Broström M, et al. Ash transformation chemistry during combustion of biomass. Energy Fuels 2012;26:85–93. https://doi.org/10.1021/ef201205b.

[60] Pfeifer C, Koppatz S, Hofbauer H. Steam gasification of various feedstocks at a dual fluidised bed gasifier: impacts of operation conditions and bed materials. Biomass Conversion and Biorefinery 2011;1:39–53. https://doi.org/10.1007/s13399-011-0007-1.

[61] Ng WC, You S, Ling R, Gin KY-H, Dai Y, Wang C-H. Co-gasification of woody biomass and chicken manure: syngas production, biochar reutilization, and cost-benefit analysis. Energy 2017;139:732–42. https://doi.org/10.1016/j.energy.2017.07.165.

[62] Pandey DS, Kwapinska M, Gómez-Barea A, Horvat A, Fryda LE, Rabou LPLM, et al. Poultry litter gasification in a fluidized bed reactor: effects of gasifying agent and limestone addition. Energy Fuels 2016;30:3085–96. https://doi.org/10.1021/acs.energyfuels.6b00058.

[63] Horvat A, Shankar Pandey D, Kwapinska M, Mello BB, Gómez-Barea A, Fryda LE, et al. Tar yield and composition from poultry litter gasification in a fluidised bed reactor: effects of equivalence ratio, temperature and limestone addition. RSC Adv 2019;9:13283–96. https://doi.org/10.1039/C9RA02548K.

[64] Ahlström JM, Alamia A, Larsson A, Breitholtz C, Harvey S, Thunman H. Bark as feedstock for dual fluidized bed gasifiers-Operability, efficiency, and economics. Int J Energy Res 2019;43:1171–90. https://doi.org/10.1002/er.4349.

[65] Karl J, Pröll T. Steam gasification of biomass in dual fluidized bed gasifiers: a review. Renew Sustain Energy Rev 2018;98:64–78. https://doi.org/10.1016/j.rser.2018.09.010.

[66] Roine A. HSC chemistry [software]. Pori: outotec, pori. 2018. Software available at: www.outotec.com/HSC.

[67] Benedikt F, Kuba M, Schmid JC, Müller S, Hofbauer H. Assessment of correlations between tar and product gas composition in dual fluidized bed steam gasification for online tar prediction. Appl Energy 2019;238:1138–49. https://doi.org/10.1016/j.apenergy.2019.01.181.

[68] Berdugo Vilches T, Maric J, Knutsson P, Rosenfeld DC, Thunman H, Seemann M. Bed material as a catalyst for char gasification: the case of ash-coated olivine activated by K and S addition. Fuel 2018;224:85–93. https://doi.org/10.1016/j.fuel.2018.03.079.

[69] Knutsson P, Maric J, Knutsson J, Larsson A, Breitholtz C, Seemann M. Potassium speciation and distribution for the K2CO3 additive-induced activation/deactivation of olivine during gasification of woody biomass. Appl Energy 2019;248:538–44. https://doi.org/10.1016/j.apenergy.2019.04.150.

[70] Faust R, Sattari M, Maric J, Seemann M, Knutsson P. Microscopic investigation of layer growth during olivine bed material aging during indirect gasification of biomass. Fuel 2020;266:117076. https://doi.org/10.1016/j.fuel.2020.117076.

[71] Marinkovic J, Thunman H, Knutsson P, Seemann M. Characteristics of olivine as a bed material in an indirect biomass gasifier. Chem Eng J 2015;279:555–66. https://doi.org/10.1016/j.cej.2015.05.061.

[72] Chr Christodoulou, Grimekis D, Panopoulos KD, Pachatouridou EP, Iliopoulou EF, Kakaras E. Comparing calcined and un-treated olivine as bed materials for tar reduction in fluidized bed gasification. Fuel Process Technol 2014;124:275–85. https://doi.org/10.1016/j.fuproc.2014.03.012.

[73] Kuba M, Fürsatz K, Janisch D, Aziaba K, Chlebda D, Łojewska J, et al. Surface characterization of ash-layered olivine from fluidized bed biomass gasification. Biomass Conv Bioref 2020. https://doi.org/10.1007/s13399-020-00863-2.

[74] Kuba M, Hofbauer H. Experimental parametric study on product gas and tar composition in dual fluid bed gasification of woody biomass. Biomass Bioenergy 2018;115:35–44. https://doi.org/10.1016/j.biombioe.2018.04.007.